Structure and Property Gradation from Surface to Bulk of Poly(L-lactic acid)/Poly(D-lactic acid) Blended Films as Estimated from Nanoscratch Tests Using Scanning Probe Microscopy

Masaki Kakiage,[†,†] Tomoyuki Ichikawa,[†] Takeshi Yamanobe,[†] Hiroki Uehara,[*,†] and Daisuke Sawai[⊥,§]

Department of Chemistry and Chemical Biology, Gunma University, Kiryu, Gunma 376-8515, Japan, and Department of Applied Chemistry, Tokyo University of Science, Shinjuku-ku, Tokyo 162-0826, Japan

ABSTRACT Structure and property gradation from surface to bulk of poly(L-lactic acid)/poly(D-lactic acid) (PLLA/PDLA) blended films was estimated from nanoscratch tests using scanning probe microscopy (SPM). The PLLA/PDLA blended film was prepared by melting, following isothermal crystallization at 150 °C due to the formation of stereocomplex crystal (sc-crystal). Grazing-incidence X-ray diffraction measurements revealed that the fraction of sc-crystal on the surface was higher than that of bulk. Two types of morphologies were observed in an SPM nanoscratch test conducted under a higher applied load: a less-deformed morphology and a plowed-up morphology. These results demonstrate that a hierarchical structure with an sc-microcrystallite networked surface could be developed by optimizing the processing conditions.

KEYWORDS: poly(lactic acid) (PLA) • stereocomplex crystal • surface functionalization • hierarchical structure • grazing-incidence X-ray diffraction (GIXD) measurement • scanning probe microscopy (SPM) nanoscratch test

INTRODUCTION

Poly(lactic acid) (PLA) has become attractive because it can be produced from a renewable resource. PLA has two optical isomers, i.e., poly(L-lactic acid) (PLLA) and poly(D-lactic acid) (PDLA), because of its asymmetric carbon atoms. An equimolar racemic blend of PLLA and PDLA produces a stereocomplex crystal (sc-crystal), in which both chains are alternately packed within a lattice cell (1−5). One of the most characteristic properties of this sc-crystal is its high melting temperature (T_m) of around 220 °C. In contrast, the usual α-form composed of pure PLLA or PDLA chains, which are separately crystallized even for blends, has a lower T_m of 170 °C. The sc-crystal also has superior resistance to hydrolysis decomposition (6), which is a principal disadvantage of general PLLA materials (7). If the formation of the sc-crystal can be controlled, there is a possibility of overcoming this disadvantage of PLLA materials.

The crystalline structure of PLLA/PDLA blended material is influenced by the molecular weight and the crystallization conditions. Little sc-crystal is formed from blending high molecular weight (HMW; >1 × 10^5) PLLA and PDLA materials (8−10). Consequently, conventional sc-crystallization is unsuitable for PLA materials since the molecular weight required for sc-crystallization is lower than that required for sufficient mechanical properties (10). A high composition of sc-crystal can be achieved by crystallization under a nonequilibrium state such as tensile drawing (11, 12) or annealing of an oriented sample (13−16), even if both PLLA and PDLA materials have HMWs (11, 13, 15), because the chains are brought into close contact by drawing. A film surface region in a nonequilibrium state is expected to preferentially support characteristic sc-crystallization because the glass transition temperature of a thin polymer film surface is lower than that of the bulk material (17) and the contact frequency between PLLA and PDLA chains is higher than in bulk because of higher chain mobility. If the sc-crystals selectivity cover an HMW-PLA film surface using a lower amount of PDLA content, there will be a number of advantages for preparing functional PLA material, since PDLA material is more expensive than PLLA. Thus, technology for controlling composition on the surface is key to developing of PLA applications.

Scanning probe microscopy (SPM) is one possible analytical technique for evaluating surface structures and properties. In particular, nanoscratch tests using SPM (18−27) enable us to determine the structure and property layering or gradation within an intermediate region from surface to

* Corresponding author. E-mail: uehara@chem-bio.gunma-u.ac.jp.
Received for review December 16, 2009 and accepted February 8, 2010
† Gunma University.
‡ Present address: Department of Applied Chemistry, Saitama University, 255 Shimo-Okubo, Sakura-ku, Saitama 338-8570, Japan.
§ Tokyo University of Science.
⊥ Present address: Synthetic Organic Chemistry Laboratories, FUJIFILM Co., Minamiashigara, Kanagawa 250-0193, Japan.
DOI: 10.1021/am900896q

bulk states of polymeric materials. We previously reported that the effects of molecular weight (28), chemical composition (29), molecular anisotropy (30), and molecular segregation (31) on polymer film surfaces have been evaluated by SPM nanoscratch tests. This SPM nanoscratch technique can evaluate the surface deformation properties from the resultant scratch patterns. The obtained data give us accurate information on surface properties with higher reproducibility.

Recently, grazing-incidence X-ray diffraction (GIXD) measurement has been widely used to identify surface crystalline structures (32−34). When the incident angle (α_i) of an X-ray beam projected onto the sample surface is equal to or smaller than the critical angle (α_c), the incident X-rays undergo total external reflection and penetrate into the sample as evanescent waves, reflecting only the surface structure. However, the spatial resolution of GIXD measurements is poor because the incident area is inevitably larger. In contrast, the SPM nanoscratch test in this study, which estimates the morphological deformation on a nano-order level, achieves extremely high resolution. Moreover, superior depth resolution is also achieved, obtaining the structure and property gradation within several tens of nanometers (31). Therefore, the structural development mechanism of the PLLA/PDLA blended film surface, including the sc-crystal, was comprehensively interpreted by combining an SPM nanoscratch test and GIXD measurement. In this study, amorphous, α-form, and sc-crystal in PLA film surfaces were identified based on surface-deformation characteristics estimated from SPM nanoscratch tests and GIXD measurements.

EXPERIMENTAL SECTION

Initial Materials. A PLLA material (LACEA, Mitsui Chemicals, Inc.; weight-average molecular weight (M_w) = 2.2×10^5, average-number molecular weight (M_n) = 1.3×10^5) and a PDLA material (Purac Japan; $M_w = 2.3 \times 10^5$, $M_n = 1.4 \times 10^5$) were used in this study. The M_w values for the two materials were almost the same. The specific optical rotation measured in chloroform at 25 °C and at a wavelength of 589 nm ($[\alpha]_D$) was −154° for PLLA material and +155° for PDLA material, suggesting that the optical purity of both of these samples was 99.5%. PLLA and PDLA materials were used after removal of the oligomer and the polymerization catalyst (stannous octoate). Before the polymer solution was prepared, both materials were dried at 100 °C for 24 h in a vacuum. Polymer solutions of 1 wt % PLLA and PDLA were prepared separately by dissolving the requisite amount of the polymer in chloroform at room temperature (RT). The solutions were admixed by vigorous stirring to prepare a solution of an equimolar blend of PLLA and PDLA as a PLLA/PDLA blended sample, in order to produce a complete mixture of PLLA and PDLA molecular chains. The PLLA and prepared PLLA/PDLA solutions were cast onto a Petri dish and covered with aluminum foil with holes, followed by solvent evaporation at RT for 5 days.

Sample Film Preparation. Two kinds of pure PLLA films and a PLLA/PDLA blended film were prepared under different crystallization conditions in this study. The obtained cast films were sandwiched between polyimide (PI) films, and the assembly was placed between a pair of hot plates installed in a vacuum chamber. The PI film, supplied by Ube Industries, Ltd. (UPILEX 125S), is desirable for preparing films that will be nanoscratched later because it has a superior flat surface (unevenness of less than 6 nm). Here, subsequent film preparation processes (melt holding, compression molding, and isothermal crystallization) were performed in a vacuum using a special molding chamber from Baldwin Co., Ltd., Tokyo (35), to inhibit thermal decomposition. Two independent pressing machines are installed in this vacuum chamber, one for melt holding and compression molding and the other for isothermal crystallization. After the atmosphere in the chamber was evacuated, the hot plates were heated to 250 °C, a sufficient temperature for melting the initial sc-crystals, and held for 4 min, followed by compression molding at 3 MPa for 1 min. One pure PLLA sample was immediately quenched in liquid nitrogen to prepare an amorphous film (PLLA-Q film). The other was isothermally crystallized at 100 °C (PLLA-100 film), at which temperature the crystallization rate of the α-form is high (36, 37). A PLLA/PDLA blended sample was isothermally crystallized at 150 °C (PLLA/PDLA film). This isothermal crystallization temperature (T_c) of 150 °C was suitable for sc-crystallization of this PLLA/PDLA blended sample, as confirmed by differential scanning calorimetry (DSC) and X-ray measurements (see Figure S1 in the Supporting Information). The PLLA-100 and PLLA/PDLA samples were compression molded at each T_c and 3 MPa for 1 h, followed by slow cooling to RT. The prepared film was 100 μm thick. The M_w values of these obtained films were unchanged even after molding, as confirmed by gel permeation chromatography (GPC) measurements (see Table S1 in the Supporting Information).

SPM Nanoscratch Tests. The SPM used in this study was an SPA400 controlled by an SPI3800N (SII NanoTechnology Inc.). This SPM system is equipped with an Olympus triangle cantilever with a spring constant of 0.57 N/m. An Si_3N_4 tip with a 30 nm radius was provided at the rear of the top of the cantilever. All SPM measurements were made at RT in a flow of dry nitrogen that reduced the humidity to less than 20%. As a first scan, the SPM tip was pushed onto the film surface with applied loads of 10 to 50 nN, and the surface was subsequently scratched with 256 lines within a $1 \times 1\ \mu m^2$ area with the load applied. These scratches were made by repeating left-to-right and right-to-left scans for the whole series of topographical images depicted in this study. After this multiline scratching, a second scan was made at a low applied load (below 1 nN) without any deformation within a $1.5 \times 1.5\ \mu m^2$ area, including the first scratched area. Scratch and scan directions were always perpendicular to the longitudinal axis of the cantilever axis, and the velocities were set to 1 μm/s.

GIXD Measurement. GIXD measurements were preformed using a Rigaku Ultima III operating at 40 kV and 40 mA with nickel-filtered Cu Kα radiation at RT. α_i values of 0.05 and 1.0° were chosen for the surface- and bulk-sensitive measurements because the α_c of PLA is 0.17° under these experimental conditions. The scan was carried out in the 2θ range of 5 to 30° with an angle interval of 0.02° and a scan speed of 0.2°/min.

RESULTS AND DISCUSSIONS

First, SPM nanoscratch tests were performed for two pure PLLA films formed under different crystallization conditions in order to estimate the standard morphological changes of amorphous and crystalline films. Figure 1 presents topographical images of the scratched surfaces of the PLLA-Q film prepared by quenching. The PLLA-Q film is a completely amorphous sample, as confirmed by GIXD measurement (see Figure S2 in the Supporting Information). Nanoperiodic patterned structures perpendicular to the sliding direction are observed on the surface of the scratched PLLA-Q film. The periodic pattern becomes clear with an increase in the applied load. Such deformation is also observed in the SPM nanoscratch test of polystyrene, a typical amorphous polymer (28). Figure 2 presents topographical images of the

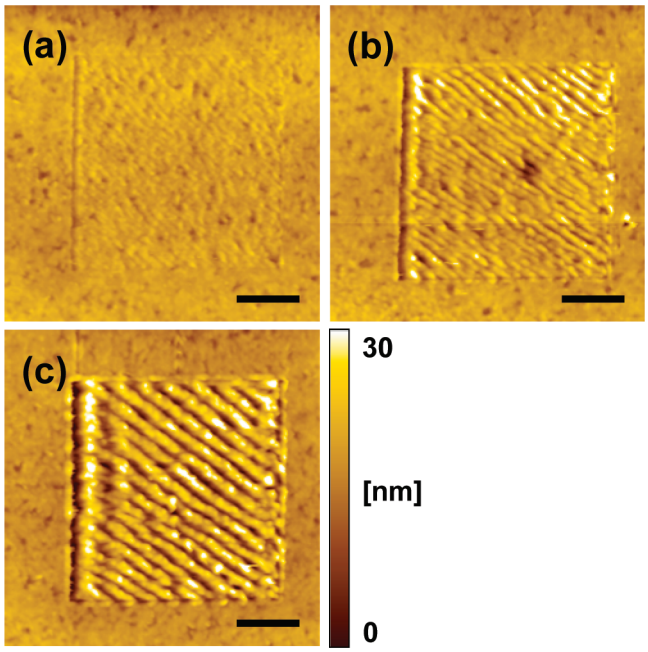

FIGURE 1. SPM topographical images of the scratched surfaces for PLLA-Q film. Nanoscratches were made at applied loads of (a) 10, (b) 30, and (c) 50 nN in the horizontal direction. Left-to-right and right-to-left scratches were produced within a central $1 \times 1\ \mu m^2$ area at an applied load. Scan size is $1.5 \times 1.5\ \mu m^2$. All scale bars are 300 nm.

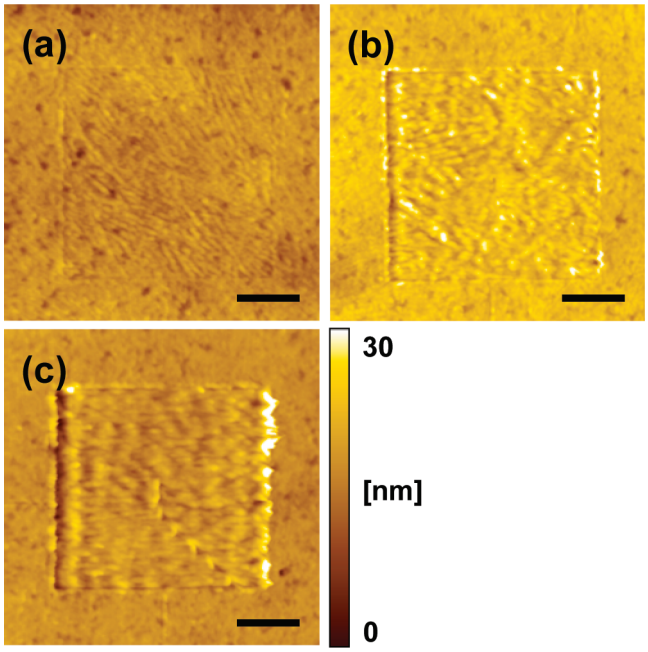

FIGURE 2. SPM topographical images of the scratched surfaces for PLLA-100 film. Nanoscratches were made at applied loads of (a) 10, (b) 30, and (c) 50 nN in the horizontal direction. Scan size is $1.5 \times 1.5\ \mu m^2$. All scale bars are 300 nm.

scratched surfaces of a PLLA-100 film isothermally crystallized at 100 °C for 1 h. The crystallinity of the PLLA-100 film was 40%, as evaluated by the area of the GIXD profile, and no difference in the crystallinity between surface and bulk was recognized (see Figure S3 in the Supporting Information). Linear structures without periodicity are observed on the surface of the scratched PLLA-100 film. This morphology is reflected in the initial lamellar structure of the film. The

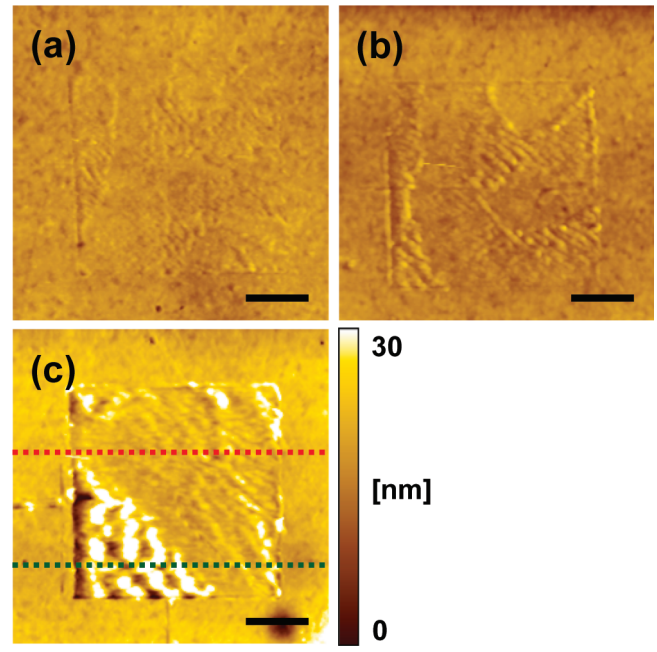

FIGURE 3. SPM topographical images of the scratched surfaces for PLLA/PDLA film. Nanoscratches were made at applied loads of (a) 10, (b) 30, and (c) 50 nN in the horizontal direction. Scan size is $1.5 \times 1.5\ \mu m^2$. All scale bars are 300 nm. Red (green) dotted lines indicate the less-deformed (plowed-up) regions.

obtained radial pattern can be considered as edge-on lamellar crystals in spherulite. This morphology is emphasized by a nanoscratch test with an increase in the applied load. Furthermore, the characteristic fibrillar structure normal to the sliding direction is observed at an applied load of 50 nN. Such a fibrillar structure is similar to the nanoscratch pattern of a uniaxially oriented film surface (30). Thus, molecules of the film surface were oriented by scratching. The scratch depth, determined from a cross-sectional profile of topographical images for the PLLA-100 film, is less than that for the PLLA-Q film (see Figure S4 in the Supporting Information). This result indicates that surface deformation is suppressed by crystallization. Furthermore, the scratch depth increases linearly with increases in the applied load, meaning that a uniform morphology is formed from surface to bulk for PLLA-Q and PLLA-100 films.

This nanoscratch test was also performed for PLLA/PDLA film isothermally crystallized at 150 °C for 1 h in order to evaluate the effect of sc-crystal on surface deformation. The crystallinity of this PLLA/PDLA film was 47% including the sc-crystal evaluated by the area of the GIXD profile (see Figure S5 in the Supporting Information). Figure 3 presents topographical images of the scratched surfaces of the PLLA/PDLA film. For scratch tests at applied loads of <30 nN, the observed morphology is similar to that for the PLLA-100 film. Linear structures expanding radially and reflecting the edge of a lamellar crystal in spherulite are observed. In contrast, an entirely different morphology is observed for PLLA/PDLA film at an applied load of 50 nN. There are two types of scratched morphologies: a less-deformed morphology (Figure 3c, red dotted line) and a plowed-up morphology (Figure 3c, green dotted line). The morphology of a less-deformed region coincides with that for the PLLA-100 film. In contrast,

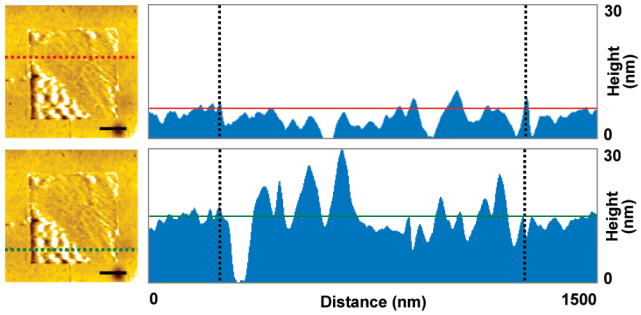

FIGURE 4. Topographical images of (left) scratched surfaces and (right) cross-sectional profiles of PLLA/PDLA film at an applied load of 50 nN. There are two types of morphologies: less-deformed (top) and plowed-up (bottom). Cross-sectional profiles of the less-deformed and plowed-up regions were extracted along the dotted red and green lines in the set of left-hand images from each left-to-right scan. Black dotted and solid lines in the right-hand column indicate the scratched region in the left images and the unscratched surface height, respectively. All scale bars are 300 nm.

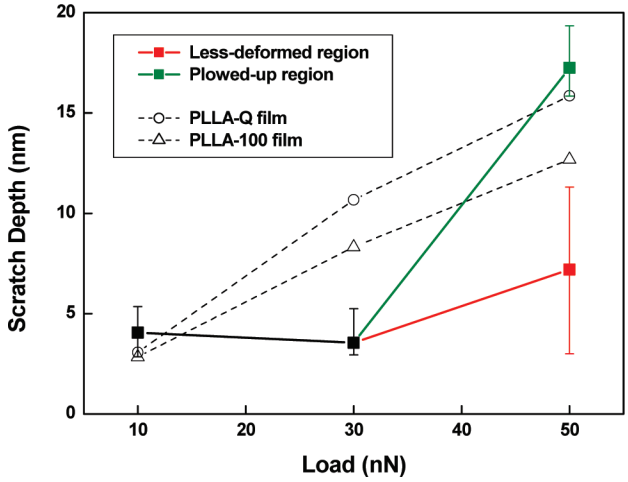

FIGURE 5. Changes in scratch depth of PLLA/PDLA film as a function of the applied load, determined from the cross-sectional profile. Red (green) plots correspond to the less-deformed (plowed-up) regions in Figure 4. Corresponding data of PLLA-Q and PLLA-100 films (see Figure S4 in the Supporting Information) were again denoted here for comparison.

the morphology of a plowed-up region has a rough surface, which is similar to that for the PLLA-Q film, but without periodicity, suggesting a complicated structure is formed in this plowed-up region. Figure 4 depicts cross-sectional profiles extracted along the red (less-deformed) and green (plowed-up) dotted lines in Figure 3c. The deep scratch and high plowed-up areas are recognized in the cross-sectional profile of the plowed-up region (Figure 4, bottom column), although the surface roughness is low, around several nanometers relative to the initial surface level, in that of the less-deformed region (Figure 4, top column). The deep scratch at the left edge of the scratched area is thought to be due to a coefficient of static friction that exceeds the coefficient of dynamic friction (31).

These surface deformations were quantitatively analyzed by comparing the scratch depths determined from the cross-sectional profiles. The scratch depths for the PLLA/PDLA film are plotted in Figure 5 as a function of the applied load. In this analysis, 10 cross-sectional profiles were extracted from each topographical image, from left to right along the scratch direction, and the recorded maximum depths were averaged and plotted as the scratch depth. The scratch depth at an applied load of less than 30 nN for the PLLA/PDLA film is less than that for PLLA-Q and PLLA-100 films. Notably, a shallower scratch depth is maintained at an applied load of 30 nN for the PLLA/PDLA film, although a linear increase in scratch depth is observed for the PLLA-Q and PLLA-100 films. This means that the surface of the PLLA/PDLA film is more robust than that of the PLLA-100 film containing only α-form. Furthermore, a drastic change in scratch depth occurs beyond an applied load of 30 nN. Specifically, the plowed-up region exhibits a deeper scratch and the less-deformed region exhibits a shallower scratch at an applied load of 50 nN. The existence of two scratch patterns reveals that the PLLA/PDLA film forms a hierarchical structure from surface to bulk. It is assumed that these nanoscratch characteristics are closely related to the crystalline structure of the film surface. For detailed analyses of the crystalline structures for surface and bulk, a sc-crystal index ($\mathbf{X}_{sc/\alpha}$) and a full width at half-maximum (FWHM) of $(110)_\alpha$ and $(110)_{sc}$ reflection peaks were evaluated from the GIXD profiles obtained at α_i values of 0.05°, for detecting surface, and 1.0°, for detecting bulk, as seen in Figure S5 in the Supporting Information. The $\mathbf{X}_{sc/\alpha}$s for each α_i value is evaluated from eq 1.

Table 1. Sc-Crystal Indexes ($\mathbf{X}_{sc/\alpha}$) and FWHMs of $(110)_\alpha$ and $(110)_{sc}$ Reflection Peaks for the Surface and Bulk of PLLA/PDLA Film

			FWHM (deg)[b]	
α_i	sensitive position	$\mathbf{X}_{sc/\alpha}$ (%)[a]	$(110)_\alpha$	$(110)_{sc}$
0.05	surface	0.36	0.45	0.90
1.0	bulk	0.18	0.42	0.67

[a] Evaluated from eq 1. [b] Evaluated from GIXD profiles in Figure S5 in the Supporting Information.

$$X_{sc/\alpha} = \frac{I(110)_{sc}}{I(110)_{sc} + I(110)_\alpha} \quad (1)$$

$I(110)_\alpha$ and $I(110)_{sc}$ indicate the integral intensities of the $(110)_\alpha$ and $(110)_{sc}$ reflection peaks. The obtained $\mathbf{X}_{sc/\alpha}$ and FWHMs for the PLLA/PDLA film are summarized in Table 1. The $\mathbf{X}_{sc/\alpha}$ of the surface is higher than that of the bulk, meaning that the sc-crystal is located more on the surface than in the bulk. Therefore, the sc-crystal successfully concentrates on the surface for the PLLA/PDLA film under these preparation conditions. This result demonstrates that the characteristic nanoscratch behavior of PLLA/PDLA film is attributable to the existence of sc-crystal segregated on the film surface. The crystalline size of the sc-crystal estimated by FWHM is less in the surface than in the bulk, but the α-form is almost the same. The plasticizer content (38) or lower molecular weight (LMW) component (31) is known to segregate on a polymer film surface, and an sc-crystal is known to form preferentially by blending LMW-PLLA and PDLA materials (8−10). Thus, it is reasonable that an sc-crystal can be formed well on a surface that is in a nonequilibrium state.

The nanoscratch test using SPM revealed that PLLA/PDLA film has a hierarchical structure, in which the surface region (~5 nm) has improved wear resistance. Considering that the sc-crystal is located more on the surface of this PLLA/PDLA film, the surface properties develop due to the existence of an sc-crystal. However, the fraction of sc-crystal located on the surface of this PLLA/PDLA film is at most 40% in a totally crystalline component. Moreover, the crystalline size of sc-crystal is smaller than bulk. These results indicate that the reason the mechanical properties develop on the surface of PLLA/PDLA film is not sc-crystal formation alone. The development of mechanical properties (11, 12, 39) and hydrolysis resistance (6) in PLLA/PDLA are explained by the formation of networks between sc-microcrystallites. A similar sc-microcrystallite network is formed on our PLLA/PDLA film surface. Therefore, scratch deformation of the PLLA/PDLA film is suppressed. In contrast, a plowed-up region is recognized as having less of an sc-microcrystallite network. The scratch depth for a plowed-up region is greater than that for PLLA-100 film, which contains only α-form. Here, an sc-crystal acts as a nucleating agent for α-form crystallization (40−43) due to the higher crystallization rate (44) and/or the stronger interaction between PLLA and PDLA molecules (45). At the same time, the addition of PDLA leads to a reduction in crystalline size because the stronger PLLA/PDLA interaction restricts the mobility of PLLA chains (8, 40, 46). The crystalline size change induces a difference in scratch depth between PLLA homopolymer and PLLA/PDLA blended samples. These results demonstrate that the morphology and deformation characteristics of the PLLA/PDLA film surface are dominated by the structural effect of sc-crystal. The surface of PLLA/PDLA film exhibits superior wear resistance because of its sc-microcrystallite networked structure. In contrast, it is plowed-up at higher applied loads in areas where this sc-microcrystallite network is diluted. Hence, the hierarchical structuring in the surface arises from the sc-microcrystallite network density gradation from surface to bulk localized to a small surface region (~20 nm), as effectively evaluated by SPM nanoscratch testing.

It is difficult to form sc-crystal by blending HMW-PLLA and PDLA materials (8−10), especially in a molten state (9, 10). However, this methodology is important for industry. We attempted to induce sc-crystallization only in the surface region, which is in a nonequilibrium state, using HMW materials (>1 × 10^5) in a molten state and considering the chain diffusion and contact frequency, the predominant factors in sc-crystallization (8, 47, 48), using only optimization of the processing conditions, i.e., T_m and T_c. Consequently, we were able to prepare PLLA/PDLA film with the characteristic sc-microcrystallite networked structure only on the surface. The structure and property gradations from surface to bulk of PLLA/PDLA film are developed by controlling molecular diffusion in the molten state (T_m) and by selective sc-crystallization only on the surface (T_c). It is also important that this hierarchy can assign a different role to surface and bulk. The surface has a function, i.e., heat and hydrolysis resistance, and the bulk provides the overall mechanical properties. Therefore, this PLLA/PDLA film, with its structure and property gradation, is one approach for developing a single polymer composite material with specific economic and environmental benefits.

CONCLUSIONS

The surface structure of PLLA/PDLA blended film was investigated using an SPM nanoscratch test. A shallower scratch was maintained under an applied load of 30 nN for the PLLA/PDLA film, indicating that the surface of the PLLA/PDLA film was more robust than that of the pure PLLA film. Two scratched morphologies were observed at higher applied loads: a less-deformed morphology and a plowed-up morphology. Considering the fraction of sc-crystal on the surface was higher than that of bulk, as evaluated by GIXD measurements, these surface characteristics were attributed to the existence of sc-crystal. Specifically, a hierarchical structure with an sc-microcrystallite networked surface could be developed by optimizing the processing conditions, i.e., T_m and T_c. These results demonstrate that the surface functionalization of PLLA/PDLA film was dominated by the structural effect of sc-crystal. Such a hierarchical structure, including α-form and sc-crystal, which have the same chemical structure but different crystalline strucutres, could be recognized visually with an SPM nanoscratch test. Therefore, the SPM nanoscratch test is expected to become an evaluation technology for PLA film surfaces.

Acknowledgment. This work was partially supported by the Industrial Technology Research Grant Program from the New Energy and Industrial Technology Development Organization (NEDO) of Japan.

Supporting Information Available: Table S1, Figures S1−S5, and corresponding description of DSC, X-ray, and GPC measurements (PDF). This material is available free of charge via the Internet at http://pubs.acs.org.

REFERENCES AND NOTES

(1) Ikada, Y.; Jamshidi, K.; Tsuji, H.; Hyon, S.-H. *Macromolecules* **1987**, *20*, 904.
(2) Brizzolara, D.; Cantow, H.-J.; Diederichs, K.; Keller, E.; Domb, A. J. *Macromolecules* **1996**, *29*, 191.
(3) Tsuji, H.; Ikada, Y. *Macromol. Chem. Phys.* **1996**, *197*, 3483.
(4) Cartier, L.; Okihara, T.; Lotz, B. *Macromolecules* **1997**, *30*, 6313.
(5) Sawai, D.; Tsugane, Y.; Tamada, M.; Kanamoto, T.; Sungil, M.; Hyon, S.-H. *J. Polym. Sci., Part B: Polym. Phys.* **2007**, *45*, 2632.
(6) Tsuji, H. *Polymer* **2000**, *41*, 3621.
(7) Lunt, J. *Polym. Degrad. Stab.* **1998**, *59*, 145.
(8) Tsuji, H.; Hyon, S.-H.; Ikada, Y. *Macromolecules* **1991**, *24*, 5651.
(9) Tsuji, H.; Ikada, Y. *Macromolecules* **1993**, *26*, 6918.
(10) Kakuta, M.; Hirata, M.; Kimura, Y. *Polym. Rev.* **2009**, *49*, 107.
(11) Sawai, D.; Tamada, M.; Yokoyama, T.; Kanamoto, T.; Hyon, S.-H.; Moon, S. *Sen'i Gakkaishi* **2007**, *63*, 1.
(12) Sawai, D.; Tamada, M.; Kanamoto, T. *Polym. J.* **2007**, *39*, 953.
(13) Tsuji, H.; Ikada, Y.; Hyon, S.-H.; Kimura, Y.; Kitao, T. *J. Appl. Polym. Sci.* **1994**, *51*, 337.
(14) Takasaki, M.; Ito, H.; Kikutani, T. *J. Macromol. Sci., Part B: Phys.* **2003**, *42*, 403.
(15) Furuhashi, Y.; Kimura, Y.; Yoshie, N.; Yamane, H. *Polymer* **2006**, *47*, 5965.
(16) Zhang, J.; Tashiro, K.; Tsuji, H.; Domb, A. J. *Macromolecules* **2007**, *40*, 1049.
(17) Forrest, J. A.; Dalnoki-Veress, K.; Stevens, J. R.; Dutcher, J. R. *Phys. Rev. Lett.* **1996**, *77*, 2002.

(18) Leung, O. M.; Goh, M. C. *Science* **1992**, *255*, 64.
(19) Jing, J.; Henriksen, P. N.; Wang, H.; Marteny, P. *J. Mater. Sci.* **1995**, *30*, 5700.
(20) Khurshudov, A.; Kato, K. *Wear* **1997**, *205*, 1.
(21) Lewis, A. L.; Cumming, Z. L.; Goreish, H. H.; Kirkwood, L. C.; Tolhurst, L. A.; Stratford, P. W. *Biomaterials* **2001**, *22*, 99.
(22) Aoike, T.; Uehara, H.; Yamanobe, T.; Komoto, T. *Langmuir* **2001**, *17*, 2153.
(23) Beake, B. D.; Leggett, G. J.; Shipway, P. H. *Polymer* **2001**, *42*, 7025.
(24) Lewis, A. L.; Tolhurst, L. A.; Stratford, P. W. *Biomaterials* **2002**, *23*, 1697.
(25) Schmidt, R. H.; Haugstad, G.; Gladfelter, W. L. *Langmuir* **2003**, *19*, 898.
(26) Schmidt, R. H.; Haugstad, G.; Gladfelter, W. L. *Langmuir* **2003**, *19*, 10390.
(27) Beake, B. D.; Shipway, P. H.; Leggett, G. J. *Wear* **2004**, *256*, 118.
(28) Aoike, T.; Yamamoto, T.; Uehara, H.; Yamanobe, T.; Komoto, T. *Langmuir* **2001**, *17*, 5688.
(29) Aoike, T.; Ikeda, T.; Uehara, H.; Yamanobe, T.; Komoto, T. *Langmuir* **2002**, *18*, 2949.
(30) Uehara, H.; Asakawa, T.; Kakiage, M.; Yamanobe, T.; Komoto, T. *Langmuir* **2006**, *22*, 4985.
(31) Suwa, J.; Kakiage, M.; Yamanobe, T.; Komoto, T.; Uehara, H. *Langmuir* **2007**, *23*, 5882.
(32) Nishino, T.; Matsumoto, T.; Nakamae, K. *Polym. Eng. Sci.* **2000**, *40*, 336.
(33) Yakabe, H.; Sasaki, S.; Sakata, O.; Takahara, A.; Kajiyama, T. *Macromolecules* **2003**, *36*, 5905.
(34) Yakabe, H.; Tanaka, K.; Nagamura, T.; Sasaki, S.; Sakata, O.; Takahara, A.; Kajiyama, T. *Polym. Bull.* **2005**, *53*, 213.
(35) Uehara, H.; Miyuki, K. *Jpn. Kokai Tokkyo Koho* **2006**, 334959.
(36) Iannace, S.; Nicolais, L. *J. Appl. Polym. Sci.* **1997**, *64*, 911.
(37) Laura, M.; Lorenzo, D. *Eur. Polym. J.* **2005**, *41*, 569.
(38) Ramirez, M. X.; Hirt, D. E.; Wright, L. L. *Nano Lett.* **2002**, *2*, 9.
(39) Tsuji, H.; Ikada, Y. *Polymer* **1999**, *40*, 6699.
(40) Schmidt, S. C.; Hillmyer, M. A. *J. Polym. Sci., Part B: Polym. Phys.* **2001**, *39*, 300.
(41) Yamane, H.; Sasai, K. *Polymer* **2003**, *44*, 2569.
(42) Tsuji, H.; Takai, H.; Saha, S. K. *Polymer* **2006**, *47*, 3826.
(43) Rahman, N.; Kawai, T.; Matsuba, G.; Nishida, K.; Kanaya, T.; Watanabe, H.; Okamoto, H.; Kato, M.; Usuki, A.; Matsuda, M.; Nakajima, K.; Honma, N. *Macromolecules* **2009**, *42*, 4739.
(44) He, Y.; Xu, Y.; Wei, J.; Fan, Z.; Li, S. *Polymer* **2008**, *49*, 5670.
(45) Zhang, J.; Sato, H.; Tsuji, H.; Noda, I.; Ozaki, Y. *Macromolecules* **2005**, *38*, 1822.
(46) Tsuji, H.; Horii, F.; Hyon, S.-H.; Ikada, Y. *Macromolecules* **1991**, *24*, 2719.
(47) Tsuji, H.; Hyon, S.-H.; Ikada, Y. *Macromolecules* **1991**, *24*, 5657.
(48) Fujita, M.; Sawayanagi, T.; Abe, H.; Tanaka, T.; Iwata, T.; Ito, K.; Fujisawa, T.; Maeda, M. *Macromolecules* **2008**, *41*, 2852.

AM900896Q